Article

Carbonization of biomass in constant-volume reactors

Maider Legarra, Trevor Morgan, Scott Q Turn, Liang Wang, Øyvind Skreiberg, and Michael Jerry Antal

Energy Fuels, **Just Accepted Manuscript** • DOI: 10.1021/acs.energyfuels.7b02982 • Publication Date (Web): 29 Nov 2017

Carbonization of biomass in constant-volume reactors

Maider Legarra[a,]*, Trevor Morgan[a], Scott Turn[a], Liang Wang[b], Øyvind Skreiberg[b], and Michael Jerry Antal Jr[a,]

[a]Hawaii Natural Energy Institute, University of Hawaii at Manoa, Honolulu, HI 96822, USA

[b]SINTEF Energy Research, Sem Saelands vei 11, Trondheim, Norway

*Corresponding Author: Maider Legarra

ABSTRACT

A novel carbonization process that realizes near-theoretical fixed-carbon yields in ~3 h is presented. Norwegian spruce and birch sawdusts were carbonized in a hermetically-sealed reactor at an initial nitrogen pressure of 0.1 MPa. During a carbonization test, the reactor vessel retained all pyrolytic products inside the hot reaction zone invoking high pressures as the temperature was raised. Given the elevated partial pressures of volatiles and their extended residence times, secondary, heterogeneous, char-forming reactions between the hot solid and the tarry vapors appeared to be promoted. This resulted in charcoals with a remarkably high fixed-carbon yield, non-condensable gases mainly composed of CO_2 and negligible amount of free tars.

This work presents a reproducibility study on the experimental method and explores the effects of heat treatment temperature, particle size, mass loading and immersion time on product distributions and charcoal properties. Proximate and elemental analyses, heating values and scanning electron microscope images of charcoal are presented. Higher heat treatment

This is the accepted manuscript of an article published in Energy & Fuels.
DOI: http://dx.doi.org/10.1021/acs.energyfuels.7b02982

temperatures (from 300 to 400°C), smaller grains (from <2 to <0.2 mm), longer immersion times (from 30 to 190 min) and greater mass loadings (from 130 to 165 g of biomass per liter of reactor) intensified wood devolatilization without losing charcoal fixed-carbon yields. Final charcoal products had lower volatile matter contents and improved fixed-carbon contents. Temperature produced the strongest effect transforming the virgin spruce with a fixed-carbon content of 15% to charcoals with fixed carbon contents of 52% at 300°C and 73% at 400°C. The increase in temperature resulted in a transient plastic phase that changed the char appearance from loose, particulate matter to a smooth, shiny solid product with the appearance of coke.

1. Introduction

Since ancient times, humans have valued the unique properties of charcoal. The first recorded use dates back to the Old World, over 30,000 years ago, when humans applied charcoal as a cave pigment [1]. Several millennia later, around 8000 years ago, its use as a metallurgical reductant began [2]. The manufacturing of new metals had such a great impact on prehistoric societies that scholars traditionally divided history into Stone, Bronze and Iron ages. The use of charcoal as a reductant continued down through the centuries till now, with additional uses being discovered along the way.

Nowadays, charcoal suits a variety of applications. It is used as a fuel for cooking, barbecuing or heating, as a reductant for metal production, and as a soil amendment. With additional processing it can be activated for air and water filtration or used in supercapacitors[3-4]. The multi-

This is the accepted manuscript of an article published in Energy & Fuels.
DOI: http://dx.doi.org/10.1021/acs.energyfuels.7b02982

purpose nature of charcoal and its high demand around the globe have inspired entrepreneurs to develop carbonization units, but a lack of technical information has often led to inefficient processes that have negative impacts due to deforestation and release of harmful emissions [5-6].

Biomass carbonization processes heat virgin biomass, e.g. wood, under an inert or low-oxygen atmosphere. The biomass dries and devolatilizes leading to a final charcoal product with an increased relative carbon content and a calorific value roughly double that of the raw biomass. Traditional carbonization methods typically consisted of firing wood that had been loaded inside excavated earth pits or piled up in earth mounds covered with turf or moistened clay [4]. Under average conditions, the whole carbonization process could take weeks and yielded around 25 wt% charcoal relative to the amount of the dry wood charge [4]. The operation was so specialized that it was generally supervised by professional charcoal burners or colliers [7].

Traditional methods are still widely used today, particularly in lesser developed nations, but the continuing global demand for charcoal has led to more efficient and less labor intensive technologies [6, 8-9]. Modern industrial techniques generally use retorts for the carbonization process [10]. In a retort, the biomass is pyrolyzed under a continuous gas flow while supplying heat either internally or externally. Typical reported charcoal yields are around 34 wt% [11-12].

Achieving an increased charcoal yield has little value unless charcoal quality parameters are specified and maintained [10]. These parameters vary depending on the charcoal market. For example, the fixed-carbon (fC) content of charcoal is found to be the main characteristic required

This is the accepted manuscript of an article published in Energy & Fuels.
DOI: http://dx.doi.org/10.1021/acs.energyfuels.7b02982

by the metallurgical industry and is typically specified as ≥70% fC content [13]. Charcoal for soil amendment, or biochar, requires elemental carbon content over 50% and low concentrations of heavy metals [14].

With the aim of creating a more meaningful definition of efficiency for biocarbon production, Antal and Grønli [15] used the charcoal yield and fixed-carbon content parameters to define a new parameter, the fixed-carbon yield, determined by multiplying the pyrolysis efficiency by the relative purity of the carbon created from the dry ash-free feedstock as $y_{fC} = y_{char} \cdot \%fC/(100 - \%ash_{feed})$. The R^3 Lab at the Hawaii Natural Energy Institute (HNEI) has been conducting research on the production of charcoal with high fixed-carbon yields since ~1990. In 1851, hopes for the production of charcoal with high fixed-carbon yield flourished when Violette carbonized dry wood in a sealed vessel under pressure. He reported a charcoal that resembled coking coal with a charcoal yield of 78.7% at 320°C (vs. 29.7% at atmospheric pressure) and a carbon content of 65.6% [16]. The fixed-carbon content and peak pressure were not reported but pressures were sufficient to cause several glass reactors to explode during the experiments. Despite the promising results, no further pyrolysis under elevated pressure was performed for over a century until 1992, when Mok, Antal and co-workers [17] at HNEI confirmed the findings from Violette's research on charcoal production in a completely sealed vessel.

At present, the positive influence of pressure during carbonization is widely acknowledged.[15, 18-22] The vast majority of work on pressurized carbonization is performed in reactors that operate with a sweep gas that partially or completely remove vapors from the hot reaction zone. Research data on constant-volume carbonization (CVC), i.e. employing reactors that retain the

This is the accepted manuscript of an article published in Energy & Fuels.
DOI: http://dx.doi.org/10.1021/acs.energyfuels.7b02982

pyrolytic products in the reaction zone and lack gas flows, is limited. Constant-volume carbonization permits decoupling variables that are interrelated in other kind of reactors. For example, the effect of internal and total system pressure can be evaluated separately by the pre-addition of an external gas. The work from Mok et al. [17] on carbonization in sealed vessels reported the effects of moisture content, mass loading, biomass type and the addition of an external gas on heat of reactions and char yields. The highlights of their findings are:

- Carbonization in sealed reactors was found to be exothermic and produced high charcoal yields (40% from cellulose, 48% from *Eucalyptus gummifera*).
- Higher mass loadings (sample mass per unit reactor volume) increased the exothermic heats of reaction, expedited reaction rates, reduced reaction onset temperatures and boosted charcoal yields (fixed-carbon contents were not measured). These findings proved to be related to the sample mass loaded per unit of reactor volume rather than to the absolute sample mass.
- The concentration of the released volatiles, and not the system pressure, was identified as the key factor influencing the reported results. Adding an external gas to increase initial reactor pressure resulted in no improvement on char yields or reaction heats.
- Increasing the moisture content of cellulose from ~6 to ~27% resulted in improved charcoal yields, lower reaction onset temperatures and similar heats of reaction.
- Higher lignin contents and/or lower hemicellulose contents in the feedstock improved charcoal yields.

Unfortunately, the charcoals produced by Mok et al. were not subject to proximate analysis and the fixed-carbon yields were not calculated [17]. Subsequent pyrolysis work performed by Antal

This is the accepted manuscript of an article published in Energy & Fuels.
DOI: http://dx.doi.org/10.1021/acs.energyfuels.7b02982

and co-workers abandoned this line of work for decades. Instead, the focus was switched to pyrolysis in constant-pressure reactors operated with a sweep gas. Their work, along with extensive literature studies on pyrolysis under pressure in a variety of reactor designs, revealed the importance of secondary reactions during pyrolysis on reducing tar yields in favor of additional secondary char formation and a gas composed mainly of water, carbon dioxide, methane, hydrogen, and carbon monoxide [15]. These secondary reactions can be promoted by increasing the partial pressure of the released volatiles and by prolonging the vapor residence times. In a pressurized reactor with a gas flow, this can be achieved by the use of higher pressures, reduced flows, larger particles or lower heating rates [15, 20-21, 23]. However, the effects of constant-volume carbonization are different to those from the use of elevated pressure with a sweep gas, i.e. Flash Carbonization [TM].

The most recent work on constant-volume carbonization performed by Antal and co-workers explored the roles of temperature and pressure on product yields and properties of charcoal derived from cellulose [24-25]. Carbonization in sealed reactors reported fixed-carbon yields close to the limiting values set by thermodynamics [24-25]. Given the interesting preliminary results from constant-volume carbonization experiments, work has continued using Norwegian spruce and birch as feedstocks. The specific aim is to produce a charcoal with a high fixed-carbon yield and with low volatile matter for use in metallurgical industries. The present work presents the roles of temperature, particle size, mass loading and immersion time on product distribution and properties of the charcoals produced from CVC. Results from proximate and elemental analysis, heating values and scanning electron microscope (SEM) images are also presented.

This is the accepted manuscript of an article published in Energy & Fuels.
DOI: http://dx.doi.org/10.1021/acs.energyfuels.7b02982

2. Methods

The following sections describe the evolution of the experimental apparatus and the procedures used in carbonization experiments.

2.1 Apparatus Evolution

The carbonization reactor — referred to as the Wall Heated Tubing Bomb (WHTB) —evolved from the original model presented in references [24-25], to an intermediate single reactor model, to the current dual reactor system presented in Figure 1.

The original model was equipped with a single reactor body that could hold a maximum of 12 g of sawdust. This capacity limited the amount of char manufactured and recovered, and therefore the number of analyses that could be applied to the char. Chars manufactured in the original WHTB were only subjected to proximate analysis and occasionally to SEM. [24-25] A greater charcoal mass was desired to allow additional analyses and obtain a better understanding of the carbonization process, the char properties and potential applications.

The intermediate and current versions share the same operating principles, enabling constant-volume pyrolysis in a hermetically-sealed batch reactor able to withstand high temperatures and

This is the accepted manuscript of an article published in Energy & Fuels.
DOI: http://dx.doi.org/10.1021/acs.energyfuels.7b02982

pressures (up to 16.24 MPa at 537°C). Improvements from the original reactor include a higher loading capacity, enhanced safety, and the ability of acquiring highly reproducible data. The intermediate model increased the capacity to 14g of sawdust through internal modifications of the original reactor. The intermediate system was equipped with a single reactor body with analogous characteristics to the current WHTB described in this section. Finally, the current WHTB model doubled the active volume by adding a second reactor body.

Analysis of the char produced in the most recent WHTB reactor design include proximate and ultimate analysis, higher heating value by bomb calorimetry and SEM imaging. Ongoing work will additionally include X-ray fluorescence (XRF) spectroscopy, nuclear magnetic resonance spectroscopy (NMR), Fourier transform infrared spectroscopy (FTIR), BET surface area measurements, thermogravimetric analysis under CO_2 and N_2 (TGA-CO_2, TGA-N_2), X-ray diffraction (XRD) and transmission electron microscopy (TEM).

Each reactor body, the colored section in Figure 1, is constructed from a section of 316 stainless steel tubing that is 17.15 cm long with a 2.54 cm outer diameter and a wall thickness of 2.11 mm. This reactor has an allowable working pressure of 21.37 MPa at room temperature and 16.24 MPa at 537°C. After it is constructed and prior to use, each new reactor is hydrostatically pressure tested at 21.87 MPa. After the reactor is loaded and assembled, a leak test is also performed, prior to each experiment. Swagelok fittings and reducing unions connect the top of each reactor body to a 6.35 mm stainless steel tube referred to as the "stem" of the reactor (rated at 35.26 MPa at room temperature). At the bottom of each reactor body, the unions provide an insertion point for a type K thermocouple (TC1 and TC2 in Figure 1) whose sensing tip is

This is the accepted manuscript of an article published in Energy & Fuels.
DOI: http://dx.doi.org/10.1021/acs.energyfuels.7b02982

located on the cylinder axis and at the midpoint of each reactor body. This new way of inserting and centering the TC has improved the reliability and reproducibility of the axis temperature data. The original model measured the axis temperature with a TC inserted from the top which required the use of a TC holder (a SS tube inserted through the center of the reactor) that caused problems with the reproducibility of the temperature measurements.

Additional type K thermocouples are positioned internally at the midway point of the reactor stems (TC5 and TC6 in Figure 1) and on the outer reactor wall (TC3 and TC4 in Figure 1). A union cross connects both stems with 6.35 mm stainless steel tubing side arms. The arms are connected to the valves, burst diaphragm and other system components shown in Figure 1. The pressure transducer (Omega, model PX 602-5KGV) has a range from 0.1 to 34.58 MPa with a 1.0% accuracy (full scale) which is used in conjunction with a digital readout (Omega, model DP25-S). The burst diaphragm (Oseco STD) is rated at 16.20 MPa at 22°C in keeping with the allowable working pressure of the weakest part of the WHTB reactor (16.24 MPa at 537°C). The burst diaphragm ruptures if its rated pressure is exceeded, protecting the WHTB reactor from experiencing pressures beyond design specifications and catastrophic failure. The outlet of the burst diaphragm vents through a tube into a bucket filled with water that serves as a buffer / shock absorber to dissipate the released energy.

Prior to an experiment, the reactor body is filled with a weighed amount of biomass (spruce, birch, oak or cellulose) and a piece of stainless steel mesh is placed on top to retain solids in the reactor. During an experiment, the WHTB colored sections in Figure 1 are directly heated by a fluidized alundum sand bath (Techne, model SBL-2D) with a maximum temperature rating of

This is the accepted manuscript of an article published in Energy & Fuels.
DOI: http://dx.doi.org/10.1021/acs.energyfuels.7b02982

600°C. A diaphragm pump (Speedaire model No. 26x362) is used to deliver clean dry air to fluidize the sand bath. A rotameter is installed between the pump and the sand bath to regulate airflow (maximum specified air flow of 57 L/min). A digital temperature controller (Omega model CN77R344) maintains the sand bath temperature throughout the experiment. The installation of the pump, rotameter and temperature controller has greatly improved the stability and reproducibility of the fluidization conditions and temperature.

The whole apparatus (reactor and sand bath) is enclosed in a protective structure built with Unistrut and Lexan panels (polycarbonate). A motorized winch is located on top of the protective structure to lower the reactor into the sand bath at the start of an experiment or to raise the reactor to terminate the experiment. A cooling fan outside the rear of the protective structure cools the upper arms and pressure sensor during the experiment, as well as the reactor after the experiment is complete. Thermocouple wires exit the protective structure from the top. A total of ten type K thermocouples are connected to the WHTB to record the temperatures during an experiment; seven are shown in Figure 1 and three are placed inside the sand bath at different depths to ensure that the hot fluidized sand bed surrounding the reactor maintains a reasonably uniform temperature. Data from the thermocouples and the pressure transducer are collected with a National Instruments SCXI 1303 data acquisition module connected to a computer using LabVIEW software for real time monitoring of the experiment and for data recording.

2.2 Materials and Experimental Procedure

This is the accepted manuscript of an article published in Energy & Fuels.
DOI: http://dx.doi.org/10.1021/acs.energyfuels.7b02982

Spruce and birch were subjected to proximate analysis by ASTM E872-82(2013) [26] and ASTM E830-87(1996)[27], and ultimate analysis by ASTM E777-17[28], E775-15[29] and E778-15[30] in HNEI laboratories. For birch and spruce, three samples were subjected to proximate analysis and two samples to ultimate analysis. Oak and cellulose feedstocks were used in two isolated experiments and their characteristics are given elsewhere. [20, 24] Prior to each test, a small sample of biomass was subjected to moisture content evaluation following the standard ASTM E871-82 [31] with the following practical modifications: the sawdust stock was too small to supply a 50 g sample for moisture analysis at each WHTB test condition; therefore a 5 to 7 g of sample was used instead.

Uncertainties of the proximate and higher heating value analyses were determined using six replicated samples of a lab-standard charcoal yielding the following values: volatile matter – 21.1%±0.3%, ash – 2.3%±0.1%, fixed carbon – 76.6%±0.2%, and higher heating value – 28.1%±0.2%. All uncertainties are based on absolute percentages.

During the reactor assembly process, the feedstock and every reactor piece were weighed and recorded. 14-18 g of dry spruce or birch were spooned into each reactor body, the reactor bodies were gently tapped during the loading to help fill voids and to loosely compact the biomass. The assembled reactor was pressurized and leak tested with nitrogen.

Prior to running the experiment, the sand bath was heated until the desired heat treatment temperature was reached and stabilized (300 or 400°C). A reactor volume evaluation was

This is the accepted manuscript of an article published in Energy & Fuels.
DOI: http://dx.doi.org/10.1021/acs.energyfuels.7b02982

performed with nitrogen to determine the gas volume in the WHTB containing the biomass sample, this step also served to flush air from the system. The reactor was pressurized with nitrogen to the desired level specified for the test, and the pressure and temperature sensors were connected to the data acquisition system. The results presented herein are all from experiments started with an initial nitrogen pressure of 1 atm. The effect of using elevated pressure prior to starting an experiment was covered in previous studies [24-25] and will be explored further in future work.

In a typical experiment, the reactor was immersed into the hot sand bath at 300 or 400°C by the motorized winch. Pressure and temperature were monitored and collected in LabVIEW. Internal temperatures and pressure increased during the experiment. After reaching the planned experimental endpoint, the WHTB was removed from the hot sand bath and cooled down to room temperature with an air fan. Long experiments were terminated 190 minutes after the WHTB was submersed into the hot sand bath, while short experiments finish 10 minutes after the end of the exotherm, i.e. the exotherm was considered to end once the pressure rise had considerably slowed down (around minute 20 in Figure 2). At this point, the reactor was taken out of the sand bath. The total experimental time of the short runs was around 30 minutes. Over the course of a test, data were recorded every second in LabVIEW.

Once the reactor cooled to room temperature, the gas phase contained in the WHTB was depressurized into a water displacement vessel (WDV) and then analyzed by GC. The amount of water displaced from the WDV was weighed to calculate the final active gas volume using the ideal gas law (for additional details, see [25]). After the gases were transferred to the WDV, the

This is the accepted manuscript of an article published in Energy & Fuels.
DOI: http://dx.doi.org/10.1021/acs.energyfuels.7b02982

reactor was disassembled and the solid product (charcoal) and SS screen were carefully removed. The stainless steel was subjected to a moisture content analysis according to ASTM D1576-13 [32] at 105°C in a convection oven. The charcoal moisture content was immediately analyzed using ASTM E1756-08 [33] in a vacuum oven, instead of the convection oven specified by the standard - to prevent charcoal combustion. In order to avoid possible errors due to non-representative subsamples of the charcoal product, a total moisture content analysis was performed on the entirety of the charcoal product recovered from the reactor. This moisture content analysis result has direct influence on the measurements of charcoal yield, mass balance and fixed-carbon yield. Subsequently, the charcoal was ground ≤20 mesh (≤ 0.841 mm) using mortar and pestle, loaded into porcelain crucibles and subjected to proximate analysis according to ASTM E872-82(2013) [26] and ASTM E830-87(1996)[27]. A mill was not used to grind samples because of the limited amount of charcoal sample produced from each experiment. Note: if SEM analysis was to be performed, a small amount of un-crushed sample was separated from the bulk sample before grinding. Selected charcoal samples were sent to SINTEF Energy Research for SEM (ZEISS SUPRA-55) analysis.

3. Results and Discussion

Results of the moisture content, proximate, ultimate, and higher heating value analyses of the parent spruce and birch materials are presented in Table 1. Values are similar for both wood materials.

This is the accepted manuscript of an article published in Energy & Fuels.
DOI: http://dx.doi.org/10.1021/acs.energyfuels.7b02982

3.1 Experimental Profile

Figure 2 shows a typical experimental profile. As soon as the reactor enters the sand bath, the outer wall temperatures immediately rise followed by the axis temperature. This is expected as the heat flow is from the sand bath to the reactor wall, and then radially inward, through the porous fuel bed, toward the longitudinal axis of the reactor. This initial lag between wall and axis temperature illustrates the temperature gradient across the reactor. Similar to typical heating rates employed in slow pyrolysis of 0.1-1°C/s [3, 34-35] or flash-carbonization rates of ~1°C/s[36], the biomass in the CVC reactor experiences rates of about 1°C/s as calculated from the figure. In comparison, flash-pyrolysis rectors employ notably faster rates ranging between 10-1000°C/s[3, 34-35].

As demonstrated in Figure 2, after ~5 minutes the reactor wall temperature approaches the sand bath temperature, the reactor pressure is ~0.55 MPa and the axis temperatures is ~165°C. At this point, the rise in pressure and axis temperature accelerates, indicating the dominance of exothermic pyrolytic reactions that causes the axis temperatures to exceed the sand bath and wall temperatures. Figure 2 shows exothermic peaks of 363 and 389°C measured in the two reactors. These observations are in line with the description elsewhere of carbonization phenomena [4], where above 280°C, wood carbonization becomes exothermic. Without an external source of heat, this spontaneous breakdown is expected to stop at ~400°C.

This is the accepted manuscript of an article published in Energy & Fuels.
DOI: http://dx.doi.org/10.1021/acs.energyfuels.7b02982

In the WHTB, the exothermic temperature peak has been demonstrated to greatly vary with the mass loading (Mass $_{biomass}$ /Volume $_{reactor}$), the feedstock particle size, the heat treatment temperature and the biomass type. Higher mass loadings, greater heat treatment temperatures and smaller particles result in greater exothermic peaks and higher final pressures (see sections 3.4, 3.5 and 3.6). Increasing the pretest reactor pressure with inert gas appeared to produce no significant changes in exothermic peaks, char yields and fixed-carbon contents. [24] In line with Mok et al. observations [17], partial pressure of volatiles, and not the system pressure, seems to play the main role on the reported results.

A large diversity of wood pyrolytic enthalpies has been documented, ranging from endothermic to exothermic at the same temperature. In 1892, Chorley and Ramsay[37] observed that wood distillation became exothermic at a temperature close to 280°C. Around a decade later, Klason and co-workers [38-40] described wood pyrolysis as an exothermic process at a starting temperature of about 250°C and an end point of about 350°C. Beyond this temperature, the charcoal was observed to further decompose mainly into gas, with no production of acetic acid or wood alcohol (methanol). When charring reactions were inhibited, Milosavljevic et al. [41] reported cellulose pyrolysis to be an endothermic process with a reaction heat of ~538 J/g of volatiles evolved. This endothermic heat was speculated to include reactions' pyrolytic enthalpies associated with the release of volatiles in addition to the latent heat of vaporization of pyrolytic products such as tars. In contrast, when char formation was promoted, the process became exothermic with a heat of reaction of roughly 2 kJ/g of char formed.

This is the accepted manuscript of an article published in Energy & Fuels.
DOI: http://dx.doi.org/10.1021/acs.energyfuels.7b02982

The overall heat of reaction has been widely recognized to be the net result of exothermic reactions that favor the formation of char and endothermic reactions that enhance volatile release [15, 41-44]. Promoting charring reactions shifts the balance in favor of exothermicity. In a reactor equipped with a gas stream, long vapor residence times, low heating rates and larger particles favor char-forming over tar-forming reactions. The current work on constant-volume carbonization has shown an enhancement in char formation - and therefore greater exothermic peaks - when higher mass loadings, greater heat treatment temperatures and/or smaller particles were employed.

During the pyrolysis of beech and spruce woods in a differential scanning calorimeter, Rath et al. [42] recognized a linear correlation between the heat of reaction and the char yield, which was in turn highly dependent on the conditions of the pyrolytic process. Mok and Antal [18] arrived at the same conclusion when pyrolyzing cellulose in a tubular flow reactor under pressure embedded in a differential scanning calorimeter. With respect to the effect of biomass type, both the major chemical components (cellulose, hemicellulose and lignin) and minor components (extractives and inorganic materials) of the feedstock are responsible for the pyrolytic properties of biomass. Generally, pyrolysis of hemicellulose and lignin is depicted as an exothermic process. In contrast, cellulose pyrolysis is reported either as an endothermic or exothermic process depending on the experimental conditions [45-48]. Kilzer and Broido recognized the existence of at least three distinct processes during cellulose pyrolysis. Two competing endothermic processes associated respectively with the formation of "dehydrocellulose" and levoglucosan (major constituent of the tar), and a third exothermic process attributed to the generation of volatile

This is the accepted manuscript of an article published in Energy & Fuels.
DOI: http://dx.doi.org/10.1021/acs.energyfuels.7b02982

carbon-containing compounds and hydrogen from "dehydrocellulose" reactions, as well as inter-molecular condensations to produce char.[49]

Figure 2 suggests that equilibrium was not attained during the 190 minute experiment as indicated by the continuous rise in pressure observed from the beginning of the experiment until the end. Most of the experiments presented herein showed a similar temperature and pressure profile. Exceptionally, an experiment that carbonized small spruce particle sizes seemed to reach stability within 120 minutes indicating that small particles may speed up the carbonization process. Contrary to the recent observations, carbonization of oak sawdust and cellulose performed in the original WHTB reactor appeared to reach stability more quickly (by 10 minutes after the end of the exotherm). Further research is needed to clarify the effect of carbonization time in relation to the roles of mass loading, particle size, biomass type and external pressure on the char product.

A temperature disparity between the two reactors is evident in Figure 2, especially between the stem and wall temperatures. Also, distinctly different char moisture contents were obtained from the two reactors. These differences are generally observed but with some variability between experiments. A preferential condensation path for liquid pyrolytic products (due to one of the reactors being slightly lower than the other) could explain these observations. Nevertheless, these differences in temperature profiles and char moisture contents have a negligible effect on the char yields (dry basis), char proximate analysis and visual properties of the final char. Efforts were made to better align the positions of the two reactors in an attempt to reduce these differences.

This is the accepted manuscript of an article published in Energy & Fuels.
DOI: http://dx.doi.org/10.1021/acs.energyfuels.7b02982

3.2 Study of reproducibility

To determine the reproducibility of the data obtained from the modified WHTB reactor, five experiments with spruce as the feedstock were performed under the same experimental conditions: a heat treatment temperature of 300°C, an initial reactor nitrogen pressure of 0.1 MPa, a mass loading of around 100 g/L and an immersion time of 190 minutes. The WHTB reactor employed for this part of the study was the intermediate, single-reactor model (see section *Apparatus Evolution*). Figure 3 illustrates the product yields from the five experimental repeats performed in the single WHTB. To compare results between the intermediate single reactor and the current dual WHTB configurations, two additional experiments were carried out under the same conditions with the current system. Figure 4 compares the average values of the product yields from the five repeat experiments with the yields obtained from the two runs with the dual reactor. Error bars are calculated as the standard deviation of the repeats (Figure 4). As shown by Figures 3 and 4, solid and gas yields derived from the single WHTB have good repeatability and were comparable to the yields from the dual reactor. On the other hand, the recovered liquid yields noticeably varied between experiments. This is somewhat expected due to the difficulty in quantifying the amount of liquid produced as it is dispersed throughout the WHTB reactor system. Some of the condensate is located in the reactor tubing or WDV, some is adsorbed on the stainless steel mesh and on the surface of the char, and some is lost due to evaporation during the removal of char and disassembly of the reactor. Liquid yields in Tables 2a and 2b are calculated from the weight loss from drying the moist charcoal and the stainless steel mesh. The carbon mass balances are a more reliable measure of product recovery (compared to the liquid yield). The amount of carbon present in the feedstock prior to the experiment was

This is the accepted manuscript of an article published in Energy & Fuels.
DOI: http://dx.doi.org/10.1021/acs.energyfuels.7b02982

compared to that present in the solid charcoal and in the gas species CO_2, CO and CH_4. The carbon in both feedstock and charcoal was determined by elemental analysis and the gas composition was quantified by gas chromatography. Carbon mass balances revealed that 97.2±0.2% of the carbon weight was recovered, indicating that the reported charcoal and gas yields are highly reliable and that carbon in the free-tar accounted for <3% of the total. Nonetheless, tars may condense and adsorb to the surface of the solid charcoal in the cooling period, and would be expected to contribute to higher volatile matter content in the proximate analysis and higher C and H contents in the ultimate analysis of the final charcoal product.

If focus is placed on the solid product yields and liquid and gas yields are removed from Figures 3 and 4, the new figures (Figures 5 and 6) depict the results of proximate analysis on charcoal. The charcoal product from each reactor body of the dual WHTB was recovered and analyzed separately. As shown in Figure 6, charcoals from the dual reactor have similar proximate analysis values as the charcoal produced from the single WHTB reactor.

3.3 List of Experiments and Parity Plot

Tables 2a and 2b list the conditions and results of 18 experiments performed under an initial nitrogen pressure of 0.1 MPa. Mass loadings, reaction temperature, particle size, immersion time and feedstock are the variables that were studied in this set of experiments. A factorial experimental design was initially developed, however limitations imposed by operating conditions and safety defined the experimental program shown in the tables.

This is the accepted manuscript of an article published in Energy & Fuels.
DOI: http://dx.doi.org/10.1021/acs.energyfuels.7b02982

The mass balances indicate that product recovery is highly dependent on the experimental conditions used. In some cases up to 21% of the initial biomass on a dry basis was unrecovered.

The carbon balance typically shows that more than 95% of the carbon is accounted for in the solid and gaseous products (see Tables 2a and 2b). As mentioned earlier, this indicates that liquid is the main unrecovered product and that measurements of charcoal and gas yields are consistent. Fixed-carbon yields in Tables 2a and 2b were calculated on a dry basis as $y_{fC} = y_{char} \cdot \%fC/100$. As emphasized in the cellulosic work [24], constant-volume carbonization was able to produce a charcoal with a near-theoretical fixed-carbon yield. The limiting value predicted by thermodynamics is calculated with a STANJAN algorithm. Solid carbon, liquid H_2O and gaseous species CO, CO_2, CH_4, H_2, H_2O, NO, NO_2 are specified as model components. A routine that minimizes the free energy of the multi-phase mixture calculates the species equilibrium yields.

The use of spruce and birch confirmed the attainment of the theoretical limiting value as illustrated by the parity plot in Figure 7. It shows that in a constant-volume reactor, smaller particles, higher temperatures and longer immersion times improve fixed-carbon yield to approach limiting value. The high values obtained with smaller wood particles in this work contrast the fixed-carbon yield of 10% predicted from the pyrolysis of cellulose powder in a TGA under a N_2 flow [24].

3.4 Effect of Heat Treatment Temperature

This is the accepted manuscript of an article published in Energy & Fuels.
DOI: http://dx.doi.org/10.1021/acs.energyfuels.7b02982

Figures 8 and 9 display product yields and char proximate analyses from spruce and birch carbonization at heat treatment temperatures of 300 and 400°C under an initial nitrogen pressure of 0.1 MPa . Raising the temperature leads to a pyrolytic product richer in gas and lower in char, and a solid char with a higher fixed-carbon and less volatiles. Exothermic temperature peaks, pressures and char higher heating values (HHV) also increased with the temperature as shown in Tables 2a and 2b.

During constant-volume carbonization of cellulose, Van Wesenbeeck et al. [24] observed two contrasting char appearances depending on the processing conditions. Chars produced under temperatures and pressures above 300°C and 2.40 MPa appeared to have experienced a transient plastic phase before resolidifying into a single piece. The appearance of the final chars produced at elevated temperature and pressure changed from loose particulate matter into a smooth, shiny solid with the appearance of coke. As observed in the present work, in the same manner, chars derived from spruce and birch transitioned from granular to molten aggregates as temperature increased from 300 and 400°C. The mass loading also played a key role on the char appearance and microstructure. Higher loadings resulted in greater reactor pressures that favored the formation of a transient plastic phase.

Scanning electron microscopy was used to image two birch charcoal samples (Figures 10 and 11). The 300°C, birch charcoal presented a granular appearance that largely retained the structure of the raw wood particle. The char surface was porous, smooth and presented some cracks and openings (Figure 10). The smooth surface shown in Figure 10c is probably related to some molten carbon or condensation of tar/pitch on the char surface. In comparison, the 400°C-birch

This is the accepted manuscript of an article published in Energy & Fuels.
DOI: http://dx.doi.org/10.1021/acs.energyfuels.7b02982

charcoal revealed both discrete charcoal grains and large size charcoal block aggregates as shown in Figure 11. Similar as the grains from the 300°C charcoal, one oblong grain partially retains the structure of the raw wood particle, with clear and wide melted zones visible on the surface (Figure 11b). There are also particles with a more spherical shape and round openings on the surface which is partially attributed to release of volatiles from particles as the solid material is softening and melting. Release of volatiles causes swelling of particles and formation of small holes on particle surface. The lack of cell structure and the compact form of these particles indicate a more intense melting and occurrence of plastic transformations as they were carbonized at higher temperature.

The presence of an intermediate liquid/molten/plastic phase during pyrolysis has been reported in the past by various researchers [20, 50-55]. During the pyrolysis of cellulose in ablative reactors at 700°C, Dauenhauer et al. confirmed the presence of a momentary liquid-intermediate by using high speed photography [54-55]. The transient plastic phase observed from the WHTB experiments is intriguing and requires further study to understand how it affects the physical and chemical properties of the char. This aspect of the research is on-going.

Drawing robust conclusions on the effect of heat treatment temperature on biomass pyrolysis through comparisons of results from literature is often difficult, or impossible. Pyrolytic processes that employ external heating can suffer from a significant variation in spatial and temporal temperature gradients within the char particle and reaction zone. These distinct internal gradients and influences from the use of different reactor configurations can lead to dissimilar char yields and physical and chemical properties for chars produced at the same temperature. In

This is the accepted manuscript of an article published in Energy & Fuels.
DOI: http://dx.doi.org/10.1021/acs.energyfuels.7b02982

spite of the differences and inconsistencies found in literature, there is general agreement regarding the key role played by the heat treatment temperature on the product distribution and properties of the char. Trends of gas and char yields with changes in temperature as well as some other char properties can be discerned among researshers. Above 280°C, as the heat treatment temperature increases, a reduction of char yields, a higher degree of char devolatilization and an increase in gas yields are typically reported [4, 15, 56-58 24]. In contrast with other type of pyrolysis configurations, the reduction of volatile matter at higher temperature in a constant-volume reactor takes place while maintaining, or slightly increasing, the fixed-carbon yield[24-25]. This capability to enhance char properties without losing the valuable fixed-carbon yield is an attractive property for both char manufacturers and consumers. Nonetheless, CVC batch processes in an industrial scale under high-pressure conditions may be costly. One of the aims of the on-going research is to generate the data required to estimate production costs at larger scales to see if it will be viable on a commercial scale.

3.5 Effect of Particle Size

The pyrolysis of small oak (149-425μm) and cellulose (50-180 μm) particles in the WHTB gave hope to the possibility of producing a charcoal high in fixed-carbon content and yield from small particles[24]. Consequently, the effect of particle size on wood carbonization was studied in greater detail. Spruce wood was milled to two particle sizes: <0.2 and <2 mm. The two sizes were pyrolyzed in the WHTB and the char was subsequently analyzed. Long (runs 10 and 14, 190 min.) and short (runs 12 and 16, ~30 min.) experiments were carried out at a temperature of

This is the accepted manuscript of an article published in Energy & Fuels.
DOI: http://dx.doi.org/10.1021/acs.energyfuels.7b02982

300°C, an initial N_2 pressure of 0.1 MPa and a mass loading of around 130 g/L. The higher heating values of the charcoals were similar from all the experiments. HHV seem to present an asymptotic behavior and it is possible that the particle size difference was not large enough to produce a significant difference (see Tables 2a and 2b). However, the product yields and proximate analysis results were influenced by the particle size (Figures 12 and 13). Fixed-carbon contents improved with the use of smaller particles for both the short and long experiments. The fixed-carbon yield marginally increased from 30.4±0.6% to 32.4±0.6% when the small particles were pyrolyzed for 190 min; whereas short experiments revealed similar fixed carbon yields (26.8±0.6% vs 27.2±0.6%) for both particle sizes.Note: the total immersion time of the short experiments were slightly different, i.e. around 25 min for the smaller particles versus the 30 min for the larger particles.

Pressure and temperature profiles (not shown) measured from experiments using small and large particles are rather distinct. Pyrolyzing smaller particles produced higher final pressures, more pronounced exotherms and an acceleration of the carbonization process. When using the smaller grains, the exotherm occurred sooner after the experiment was initiated, and pressure and temperatures became stable within 120 minutes. Conversely, larger particles showed a continuous rise of pressure during the whole experimental time of 190 minutes (as in Figure 2).

The effect of particle size on pyrolysis processes has been widely reported upon, using reactors equipped with a sweep gas or where the reactor was partially or completely open to the atmosphere. [15, 20-21, 50, 59-63] In all of these cases, volatiles were removed from the reaction zone and the pyrolyzing carbon matrix, resulting in different vapor residence times depending on the

This is the accepted manuscript of an article published in Energy & Fuels.
DOI: http://dx.doi.org/10.1021/acs.energyfuels.7b02982

pyrolysis conditions and reactor configuration. Nonetheless, researchers have consistently reported that pyrolysis of larger particles produced a beneficial effect on char-forming secondary reactions. The use of larger particles imply that the particle heating rates slow down and that volatiles experience longer residence times and higher intra-particle pressures. All these effects are associated with an enhancement of secondary charring reactions when using 'open' reactor systems [15, 20-21, 59-61, 64].

The effect of particle size on the char yields and properties from the constant-volume WHTB revealed a drastically different behavior compared to those reported in previous studies. In this case, the volatiles are not being removed once they have been released from the solid char matrix. Instead, they linger in close proximity to the solid maximizing the contact time and consequently interactions between volatiles and char, which result in more intensive secondary charring reactions that would not occur (or to a lesser extent) in reactors where volatiles are removed. Smaller grains in CVC lead to an acceleration of the carbonization process, produce higher pressures, more pronounced exotherms and a more intense degree of wood devolatilization. This results in chars with a greater fixed-carbon contents and no loss of fixed-carbon yields. Further research is being performed to study the influence of particle size when using a sealed reactor (CVC) due to the potential of using small low-grade biomass such as sawdust, grasses or agricultural residues in the production of charcoals with enhanced properties.

3.6 Effect of Mass Loading

This is the accepted manuscript of an article published in Energy & Fuels.
DOI: http://dx.doi.org/10.1021/acs.energyfuels.7b02982

Preliminary carbonization experiments using spruce mass loadings of ~165 and ~130 g/L in the WHTB (runs 15 and 16) showed that a higher loading slightly improved the fixed-carbon yield and fixed-carbon content of the charcoal (Figures 14 and 15), and raised the peak pressure from ~4.6 to ~5.7 MPa. However, very small differences in HHV of produced char and measured temperature peaks were observed between experiments with different sample loadings. The HHV seems to approach an upper limit as the theoretical fixed carbon yield is approached. Regarding the similarity in temperature peaks (around 400°C), it seems that the increment of spruce mass loadings was not enough to present clear differences, and/or differences were masked by the large thermal mass of the sand bath.

An oak experiment (run 6) with a mass loading of ~125 g/L and reactor conditions of an initial atmosphere of 0.1 MPa N_2 and a heat treatment temperature of 300°C resulted in a temperature peak of 380°C versus a peak of ~310°C when using the original WHTB reactor design, a lower mass loading and similar processing conditions.

Using cellulose (run 7), a higher mass loading, 205 g/L, was possible due its small particle size and a denser fuel bed. Analogous reactor conditions of initial pressure (0.1 MPa N_2) and heat treatment temperature (300°C) resulted in a higher final pressure and temperature peak compared to experiments using a lower mass loading of ~150 g/L and the original WHTB design [24]. Temperature and pressure peaks of 552°C and ~7 MPa were recorded, as opposed to values of 365°C and 2.34 MPa reported during cellulose pyrolysis in the previous WHTB design [24]. The final char from Test 7 was highly devolatilized; a fixed-carbon content of almost 72% versus a value of 54.3% reported for the previous WHTB experiments. [24] However, fixed-carbon yields

This is the accepted manuscript of an article published in Energy & Fuels.
DOI: http://dx.doi.org/10.1021/acs.energyfuels.7b02982

realized in current and previous cellulose carbonization experiments were similar. The remarkably high cellulosic fixed-carbon content obtained in this most recent run at moderate temperature conditions was mainly associated with the higher mass loading employed in the new WHTB reactor. Both cellulose runs were carried out under analogous temperature and pressure conditions, the only differences were the mass loadings and immersion times employed. Mass loading was increased from 155 to 205 g/L and immersion time prolongued from ~30 minutes to 190 minutes. Given that the exothermic peak is independent of the immersion times used, it was found to be radically more intense for the experiment performed with a higher mass loading.

Mass loading was identified as the key parameter leading to the rise in temperature, pressure and fixed-carbon content of the cellulosic charcoal. This recent experiment with cellulose proved that attaining a charcoal product high in fixed-carbon and low in volatiles is possible at a moderate temperature of 300°C as long as the carbonization reactor is capable of withstanding the high pressures evolved during the pyrolysis reaction. Mass loading effects in the WHTB will be further explored using birch wood as feedstock. Given the higher packing density of birch versus spruce, higher mass loadings can be tested.

In 1992, Mok et al. [17] studied the effect of mass loading on the differential scanning calorimetric curves and char yields of biomass pyrolysis in sealed crucibles. They reported that higher mass loadings (sample mass per unit reactor volume) increased the exothermic heats of reaction, expedited reaction rates, reduced reaction onset temperatures and boosted charcoal yields. Higher mass loadings raised the concentration of volatiles in the reactor which led to improved char yields and more exothermic reactions. In studies using thermogravimetric analyzers, Wang

This is the accepted manuscript of an article published in Energy & Fuels.
DOI: http://dx.doi.org/10.1021/acs.energyfuels.7b02982

et al. confirmed higher yields of charcoal and fixed-carbon when larger sample masses of wood were pyrolyzed in open and closed crucibles with pinholes [50, 65]. It was concluded that the increased yields were due to greater extents of secondary charring reactions.

3.7 Effect of Immersion Time

Figures 16 and 17 show the effect of immersion times on spruce experiments at an initial N_2 pressure of 0.1 MPa and a mass loading of around 130 g/L. Prolonging the processing time from 30 to 190 minutes lead to higher charcoal and gas yields and more devolatilized charcoals. Char heating values were similar. At a carbonization temperature of 300°C (runs 12 vs 10, and 16 vs 14), fixed-carbon yields are improved by more than 10%, relative. At 400°C (runs 13 vs 11), however, a longer reaction time did not improve the fixed-carbon yields.

An intriguing aspect of these spruce experiments is their slow rates compared to cellulose experiments in the original WHTB model. For cellulose, immersion time appears to have a lesser effect on the fixed-carbon content, and pressure and temperature stabilized within tens of minutes. Contrary to those observations, spruce carbonization in the current WHTB required hours for the pressure to stabilize which is assumed to indicate that charring reactions are near completion. Pressure and temperature did not stabilize in the majority of the tests. Surprisingly, the long experiment performed with the smallest spruce grains (<0.2 mm) achieved pressure and temperature stability after about two hours, which indicates the carbonization process is accelerated by the use of smaller particles. Further research is needed to clarify the findings reported herein and to better understand the effect of temperature, particle size, biomass type, external pressure and mass loading on the carbonization processing times.

This is the accepted manuscript of an article published in Energy & Fuels.
DOI: http://dx.doi.org/10.1021/acs.energyfuels.7b02982

4. Conclusions

1. A new reactor design for biomass carbonization is presented. The reactor — referred to as the Wall Heated Tubing Bomb (WHTB) — has an internal volume of ~0.22 L, which permits spruce and birch sawdust loadings of ~30 g and ~50 g respectively and enables constant-volume pyrolysis under high temperatures and pressures in a safe and controlled manner

2. Solid and gas yields, and proximate analysis results exhibited good repeatability of ±2%, absolute. On the contrary, liquid yields showed greater variation. This was expected due to the difficulty in recovering the liquid that condenses in the tubing system of the WHTB or WDV.

3. Constant-volume carbonization of spruce and birch produced a charcoal with a fixed-carbon yield that approached the limiting value predicted by thermodynamics.

4. Raising the heat treatment temperature from 300 to 400°C during spruce and birch carbonization under an initial nitrogen pressure of 0.1 MPa improved char properties while preserving the valuable fixed-carbon yield. The charcoal was a highly devolatilized solid product, rich in fixed-carbon and with an improved higher heating value.

5. The effect of particle size on the product yields and char properties was highly influenced by the processing conditions. In sealed vessels, smaller particle sizes seem to favor char-forming secondary reactions, whereas in reactors with gas flows that remove volatiles from the hot reaction, larger particles have been found to benefit these secondary

This is the accepted manuscript of an article published in Energy & Fuels.
DOI: http://dx.doi.org/10.1021/acs.energyfuels.7b02982

reactions. In sealed vessels, volatiles that have been released into the gas phase stay in contact with the pyrolyzing solid mass which promotes additional secondary charring reactions. Smaller grains in constant-volume reactors accelerate the carbonization process and induce higher pressures, more pronounced exotherms and a greater degree of devolatilization resulting in chars with greater fixed-carbon content without loss of fixed-carbon yield.

6. Increasing the feedstock loading per liter of reactor volume raises the volatiles partial pressure enhancing secondary reactions that improve fixed-carbon yields and fixed-carbon contents of the charcoal.
7. Prolonging immersion times in the current WHTB from 30 to 190 minutes led to higher gas yields and charcoals with less volatile matter.
8. An increase in temperature transformed the final biochar product from particulate to a transient plastic phase (TPP) and solidified into a single piece resembling coke.

Acknowledgement

The Hawaii team gratefully acknowledges support from SINTEF Energi Research AS (Award Number 006356-00003) under the BioCarb+ Project and the U.S. Office of Naval Research (Award Number N00014-14-1-054). The Norway team acknowledges the financial support from the Research Council of Norway and a number of industrial partners through the project BioCarb+ ("Enabling the Biocarbon Value Chain for Energy", grant number 228726/E20).

Bibliography

1. Robens, E.; Amarasiri , S. A., Short History of Charcoal. In *Horizons in Earth Science Research.*, Veress, B.; Szigethy, J., Eds. 2011; Vol. 5, pp 355-374.
2. Agricola, G.; Hoover, H.; Hoover, L. H., *De re metallica*. Dover Publications: 1950.
3. Lohri, C. R.; Rajabu, H. M.; Sweeney, D. J.; Zurbrügg, C., Char fuel production in developing countries – A review of urban biowaste carbonization. *Renewable and Sustainable Energy Reviews* **2016,** *59*, 1514-1530.
4. Food of the United Nations. FAO Forestry Department, Agriculture Organization. Simple Technologies of Charcoal Making. *FAO FORESTRY PAPER 41* **1987**.
5. Smith, K. R.; Pennise, D. M.; Khummongkol, P.; Chaiwong, V.; Ritgeen, K.; Zhang, J.; Panyathanya, W.; Rasmussen, R. A.; Khalil, M. A. K.; Thorneloe, S. A., Greenhouse Gases from Small-scale Combustion Devices in Developing Countries. Phase III: Charcoal-Making Kilns in Thailand. *US Environmental Protection Agency, Office of Research and Development, Washington DC* **1999**.
6. Garcia-Perez, M.; Lewis, T.; Kruger, C., Methods for producing biochar and advanced biofuels in Washington State. *Washington State University, Pullman, WA* **2010**, 137.
7. Crumrin, T., Fuel for the fires: charcoal making in the nineteenth century. *Chronicle of the Early American Industries* **1994,** *47*, 35-38.
8. *Industrial Charcoal Making*. Food Agriculture Organization of the United Nations: 1985.
9. Bruckman, V. J.; Liu, J.; Uzun, B. B.; Varol, E. A., *Biochar*. Cambridge University Press: 2016.
10. *Industrial Charcoal Production. Food and Agriculture Organization of the United Nations*. 2008.
11. Grønli, M., Industrial production of charcoal. *PyNe Newsletter* **2000,** (10).

12. Nachenius, R.; Ronsse, F.; Venderbosch, R.; Prins, W., Biomass pyrolysis. *Chemical engineering for renewables conversion* **2013,** *42*, 75-139.
13. Kempegowda, R. S.; Skreiberg, Ø.; Tran, K.-Q., Biocarbonization Process for High Quality Energy Carriers: Techno-economics. *Energy Procedia* **2017,** *105*, 628-635.
14. European Biochar Certificate - Guidelines for a Sustainable Production of Biochar. European Biochar Foundation (EBC). Arbaz, Switzerland, 2016.
15. Antal, M. J.; Grønli, M., The Art, Science, and Technology of Charcoal Production. *Industrial & Engineering Chemistry Research* **2003,** *42* (8), 1619-1640.
16. Violette, M., *Ann. Chim. Phys.* **1853,** *32*, 304.
17. Mok, W. S. L.; Antal, M. J.; Szabo, P.; Varhegyi, G.; Zelei, B., Formation of charcoal from biomass in a sealed reactor. *Industrial & Engineering Chemistry Research* **1992,** *31* (4), 1162-1166.
18. Mok, W. S.-L.; Antal, M. J., Effects of pressure on biomass pyrolysis. II. Heats of reaction of cellulose pyrolysis. *Thermochimica Acta* **1983,** *68* (2), 165 - 186.
19. Antal, M. J.; Allen, S. G.; Dai, X.; Shimizu, B.; Tam, M. S.; Grønli, M., Attainment of the Theoretical Yield of Carbon from Biomass. *Industrial & Engineering Chemistry Research* **2000,** *39* (11), 4024-4031.
20. Wang, L.; Skreiberg, Ø.; Gronli, M.; Specht, G. P.; Antal Jr, M. J., Is elevated pressure required to achieve a high fixed-carbon yield of charcoal from biomass? Part 2: The importance of particle size. *Energy & Fuels* **2013,** *27* (4), 2146-2156.
21. Wang, L.; Trninic, M.; Skreiberg, Ø.; Gronli, M.; Considine, R.; Antal, M. J., Is Elevated Pressure Required To Achieve a High Fixed-Carbon Yield of Charcoal from Biomass? Part 1: Round-Robin Results for Three Different Corncob Materials. *Energy & Fuels* **2011,** *25* (7), 3251-3265.

22. Blasi, C. D.; Branca, C.; Sarnataro, F. E.; Gallo, A., Thermal Runaway in the Pyrolysis of Some Lignocellulosic Biomasses. *Energy & Fuels* **2014,** *28* (4), 2684-2696.
23. Rousset, P.; Figueiredo, C.; De Souza, M.; Quirino, W., Pressure effect on the quality of eucalyptus wood charcoal for the steel industry: A statistical analysis approach. *Fuel processing technology* **2011,** *92* (10), 1890-1897.
24. Wesenbeeck, S. V.; Higashi, C.; Legarra, M.; Wang, L.; Michael Jerry Antal, J., Biomass Pyrolysis in Sealed Vessels. Fixed-Carbon Yields from Avicel Cellulose That Realize the Theoretical Limit. *Energy & Fuels* **2016,** *30* (1), 480-491.
25. Williams, S.; Higashi, C.; Phothisantikul, P.; Wesenbeeck, S. V.; Jr, M. J. A., The fundamentals of biocarbon formation at elevated pressure: From 1851 to the 21st century. *Journal of Analytical and Applied Pyrolysis* **2014,** (0), -.
26. ASTM E872 - 82(2013), Standard Test Method for Volatile Matter in the Analysis of Particulate Wood Fuels. 2013.
27. ASTM E830-87(1996), Standard Test Method for Ash in the Analysis Sample of Refuse-Derived Fuel ASTM International: West Conshohocken, PA, 1996.
28. ASTM E777-17, Standard Test Method for Carbon and Hydrogen in the Analysis Sample of Refuse-Derived Fuel. ASTM International: West Conshohocken, PA, 2017, 2017.
29. ASTM E775-15, Standard Test Methods for Total Sulfur in the Analysis Sample of Refuse-Derived Fuel. ASTM International: West Conshohocken, PA, 2015.
30. ASTM E778-15, Standard Test Methods for Nitrogen in Refuse-Derived Fuel Analysis Samples. ASTM International: West Conshohocken, PA, 2015.
31. ASTM E871-82(2013), Standard Test Method for Moisture Analysis of Particulate Wood Fuels. 2013.
32. ASTM D1576-13, Standard Test Method for Moisture in Wool by Oven-Drying. 2013.

33. ASTM E1756 - 08(2015) Standard Test Method for Determination of Total Solids in Biomass. 2015.
34. Maschio, G.; Koufopanos, C.; Lucchesi, A., Pyrolysis, a promising route for biomass utilization. *Bioresource Technology* **1992,** *42* (3), 219-231.
35. Demirbas, A.; Arin, G., An Overview of Biomass Pyrolysis. *Energy Sources* **2002,** *24* (5), 471-482.
36. Antal, M. J. J., *; Mochidzuki, K.; Paredes, L. S., Flash Carbonization of Biomass. *Industrial & Engineering Chemistry Research* **2003,** *42* (16), 3690-3699.
37. The society of chemical industry. *Journal of the Society of Chemical Industry* **1892,** *11* (5), 393-403.
38. Klason, P.; Heidenstam, G.; Norlin, E., Untersuchungen zur Holzverkohlung. I. Die trockene Destillation der Cellulose. Z. *Angew. Chem.* **1909,** *25*, 1205.
39. Klason, P.; Heidenstam, G. V.; Norlin, E., Teoretiska undersokningar rorande kolning af ved. I. Om torrdestillation of cellulosa. *Ark. Kemi, Mineral. Geol.* **1908,** *3*.
40. Klason, P.; Heidenstam, G. V.; Norlin, E., *Arkiv for kemi miner och geologi* **1910,** *27*, 1252.
41. Milosavljevic, I.; Oja, V.; Suuberg, E. M., Thermal Effects in Cellulose Pyrolysis: Relationship to Char Formation Processes. *Industrial & Engineering Chemistry Research* **1996,** *35* (3), 653-662.
42. Rath, J.; Wolfinger, M. G.; Steiner, G.; Krammer, G.; Barontini, F.; Cozzani, V., Heat of wood pyrolysis. *Fuel* **2003,** *82* (1), 81 - 91.
43. Di Blasi, C., Modeling and simulation of combustion processes of charring and non-charring solid fuels. *Progress in Energy and Combustion Science* **1993,** *19* (1), 71-104.
44. Koufopanos, C. A.; Papayannakos, N.; Maschio, G.; Lucchesi, A., Modelling of the pyrolysis of biomass particles. Studies on kinetics, thermal and heat transfer effects. *The Canadian Journal of Chemical Engineering* **1991,** *69* (4), 907-915.

45. Roberts, A. F., The heat of reaction during the pyrolysis of wood. *Combustion and Flame* **1971,** *17* (1), 79-86.
46. Ramiah, M. V., Thermogravimetric and differential thermal analysis of cellulose, hemicellulose, and lignin. *Journal of Applied Polymer Science* **1970,** *14* (5), 1323-1337.
47. Arseneau, D. F., Competitive Reactions in the Thermal Decomposition of Cellulose. *Canadian Journal of Chemistry* **1971,** *49* (4), 632-638.
48. Alves, S. S.; Figueiredo, J. L., Pyrolysis kinetics of lignocellulosic materials by multistage isothermal thermogravimetry. *Journal of Analytical and Applied Pyrolysis* **1988,** *13* (1), 123-134.
49. Kilzer, F. J.; Broido, A., Speculations on the nature of cellulose pyrolysis. **1965**.
50. Wang, L.; Skreiberg, Ø.; Van Wesenbeeck, S.; Grønli, M.; Antal, M. J., Experimental Study on Charcoal Production from Woody Biomass. *Energy & Fuels* **2016,** *30* (10), 7994-8008.
51. Boutin, O.; Ferrer, M.; Lédé, J., Radiant flash pyrolysis of cellulose—Evidence for the formation of short life time intermediate liquid species. *Journal of Analytical and Applied Pyrolysis* **1998,** *47* (1), 13-31.
52. Lédé, J.; Blanchard, F.; Boutin, O., Radiant flash pyrolysis of cellulose pellets: products and mechanisms involved in transient and steady state conditions. *Fuel* **2002,** *81* (10), 1269-1279.
53. Lede, J.; Li, H. Z.; Villermaux, J., Pyrolysis of Biomass. In *Pyrolysis Oils from Biomass*, American Chemical Society: 1988; Vol. 376, pp 66-78.
54. Mettler, M. S.; Vlachos, D. G.; Dauenhauer, P. J., Top ten fundamental challenges of biomass pyrolysis for biofuels. *Energy Environ. Sci.* **2012,** *5*, 7797-7809.
55. Dauenhauer, P. J.; Colby, J. L.; Balonek, C. M.; Suszynski, W. J.; Schmidt, L. D., Reactive boiling of cellulose for integrated catalysis through an intermediate liquid. *Green Chemistry* **2009,** *11* (10), 1555-1561.

56. Fuwape, J. A., Carbonization of five short rotation tropical tree species. *Developments in thermochemical biomass conversion* **1997,** *1*.
57. In *Specialits' workshop on fast pyrolysis of biomass proceedings*, 1980.
58. Kosstrin, H. M., Direct formation of pyrolysis oil from biomass.
59. Kandiyoti, R.; Herod, A.; Bartle, K. D.; Morgan, T. J., *Solid fuels and heavy hydrocarbon liquids: thermal characterization and analysis*. Elsevier: 2016.
60. Stubington, J. F.; Sumaryono, Release of volatiles from large coal particles in a hot fluidized bed. *Fuel* **1984,** *63* (7), 1013-1019.
61. Suuberg, E. M. Massachussets Institute of Technology Massachussets, 1977.
62. Di Blasi, C., Kinetic and heat transfer control in the slow and flash pyrolysis of solids. *Industrial & Engineering Chemistry Research* **1996,** *35* (1), 37-46.
63. Gábor Várhegyi; Szabó, P.; Till, F.; Zelei, B.; Michael Jerry Antal, J.; Dai, X., TG, TG-MS, and FTIR Characterization of High-Yield Biomass Charcoals. *Energy & Fuels* **1998,** *12* (5), 969-974.
64. Gonenc, S.; Sunol, A. K., *Pyrolysis of Coal*. 1994.
65. Wang, L.; Skreiberg, Ø.; Gronli, M.; Specht, G. P.; Antal, M. J. J., Is Elevated Pressure Required to Achieve a High Fixed-Carbon Yield of Charcoal from Biomass? Part 2: The Importance of Particle Size. *Energy and Fuels* **2013**.

This is the accepted manuscript of an article published in Energy & Fuels.
DOI: http://dx.doi.org/10.1021/acs.energyfuels.7b02982

Figure Captions

Figure 1. Schematic of the Wall Heated Tubing Bomb (WHTB) reactor.

Figure 2. Temperature and pressure profile of a WHTB experiment with birch as the feedstock, a heat treatment temperature of 300°C and an initial nitrogen pressure of 0.1 MPa. (a) Profile of reactor body 1 and (b) Profile of reactor body 2. ● Axis temperature. ■ Sand bath temperature. ▼ Stem temperature. ▲ Wall temperature. -- Pressure.

Figure 3. Reproducibility study on the yields of char, condensates and gas products of spruce pyrolysis in the single WHTB at a heat treatment temperature of 300°C and an initial nitrogen pressure of 0.1 MPa. Negligible free tars were recovered in the experiments. Liquid yields mainly represent water content of the final moist charcoals.

Figure 4. Comparison between product yields from spruce pyrolysis experiments in the single and dual WHTB at a heat treatment temperature of 300°C and an initial nitrogen pressure of 0.1 MPa.

Figure 5. Reproducibility study on the proximate analysis of charcoals derived from spruce pyrolysis in the single WHTB at a heat treatment temperature of 300°C and an initial nitrogen pressure of 0.1 MPa.

Figure 6. Comparison between proximate analyses of charcoals derived from spruce pyrolysis experiments in the single and dual WHTB at a heat treatment temperature of 300°C and an initial nitrogen pressure of 0.1 MPa.

Figure 7. Parity plot showing experimental versus theoretical fixed carbon yields calculated with STANJAN.

Figure 8. Effect of heat treatment temperature on the yields of char, condensate and gas from spruce and birch pyrolysis at an initial N_2 pressure of 0.1 MPa.

Figure 9. Effect of heat treatment temperature on the proximate analysis of charcoal from spruce and birch pyrolysis at an initial N_2 pressure of 0.1 MPa.

Figure 10. (a) SEM image of birch charcoal from experiment at a heat treatment temperature of 300°C and an initial nitrogen pressure of 0.1 MPa, (b) and (c) zoom-in views of selected areas in (a).

Figure 11. (a) SEM image of birch charcoal from experiment at a heat treatment temperature of 400°C and an initial nitrogen pressure of 0.1 MPa, (b) and (c) zoom-in view of selected areas in (a).

Figure 12. Effect of particle size on the yields of char, condensates and gas from spruce pyrolysis at a heat treatment temperature of 300°C and an initial nitrogen pressure of 0.1 MPa.

Figure 13. Effect of particle size on the proximate analysis of charcoal from spruce pyrolysis at a heat treatment temperature of 300°C and an initial nitrogen pressure of 0.1 MPa.

This is the accepted manuscript of an article published in Energy & Fuels.
DOI: http://dx.doi.org/10.1021/acs.energyfuels.7b02982

Figure 14. Effect of mass loading on the yields of char, condensates and gas from spruce pyrolysis at a heat treatment temperature of 300°C, an initial nitrogen pressure of 0.1 MPa, immersion time of around 25 minutes and sample size of <0.2 mm.

Figure 15. Effect of mass loading on the proximate analysis of charcoal from spruce pyrolysis at a heat treatment temperature of 300°C, an initial nitrogen pressure of 0.1 MPa, immersion time of around 25 minutes and sample size of <0.2 mm.

Figure 16. Effect of immersion time on the yields of char, condensates and gas from spruce pyrolysis at an initial nitrogen pressure of 0.1 MPa.

Figure 17. Effect of immersion time on the proximate analysis of charcoal from spruce pyrolysis at an initial nitrogen pressure of 0.1 MPa.

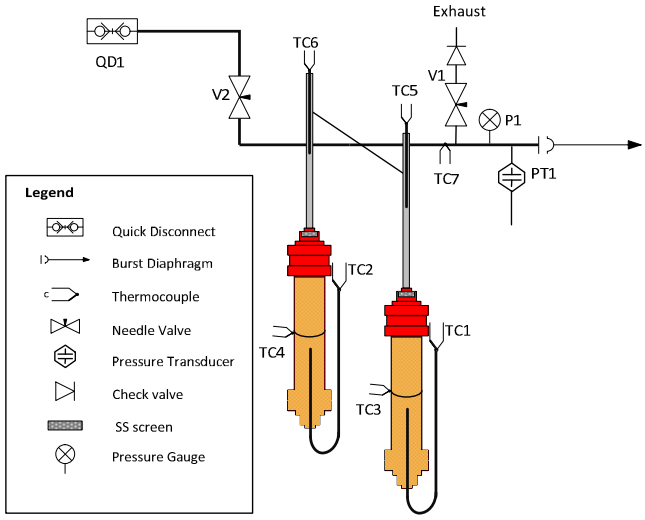

Figure 1. Schematic of the Wall Heated Tubing Bomb (WHTB) reactor.

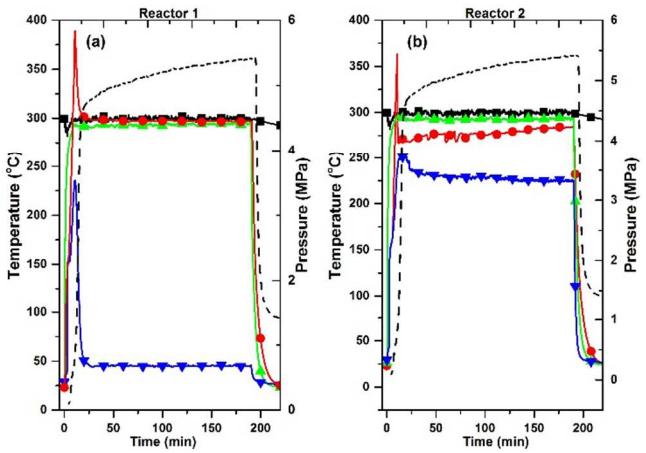

Figure 2. Temperature and pressure profile of a WHTB experiment with birch as the feedstock, a heat treatment temperature of 300°C and an initial nitrogen pressure of 0.1 MPa. (a) Profile of reactor body 1 and (b) Profile of reactor body 2. ● Axis temperature. ■ Sand bath temperature. ▼ Stem temperature. ▲ Wall temperature. -- Pressure.

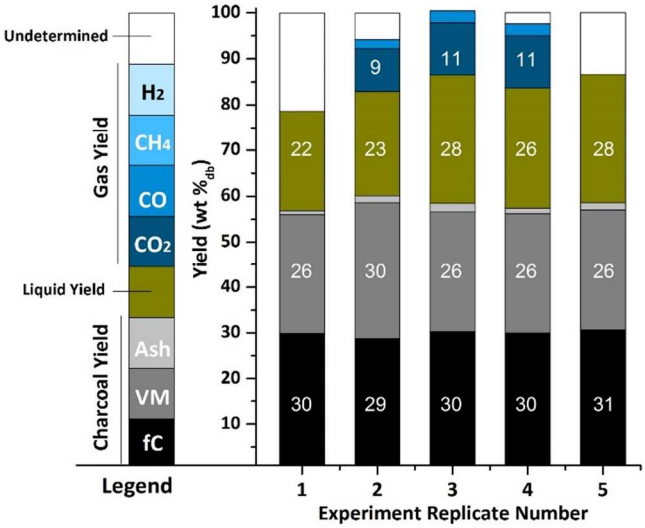

Figure 3. Reproducibility study on the yields of char, condensates and gas products of spruce pyrolysis in the single WHTB at a heat treatment temperature of 300°C and an initial nitrogen pressure of 0.1 MPa. Negligible free tars were recovered in the experiments. Liquid yield mainly represent water content of the final moist charcoal.

This is the accepted manuscript of an article published in Energy & Fuels.
DOI: http://dx.doi.org/10.1021/acs.energyfuels.7b02982

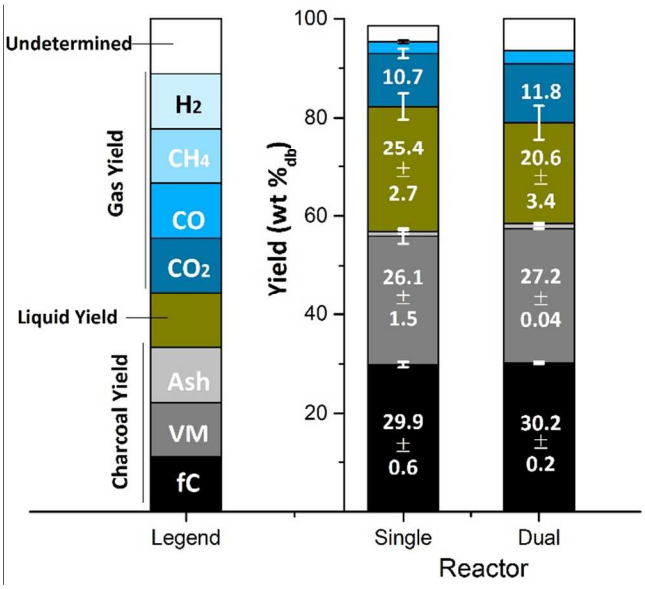

Figure 4. Comparison between product yields from spruce pyrolysis experiments in the single and dual WHTB at a heat treatment temperature of 300°C and an initial nitrogen pressure of 0.1 MPa.

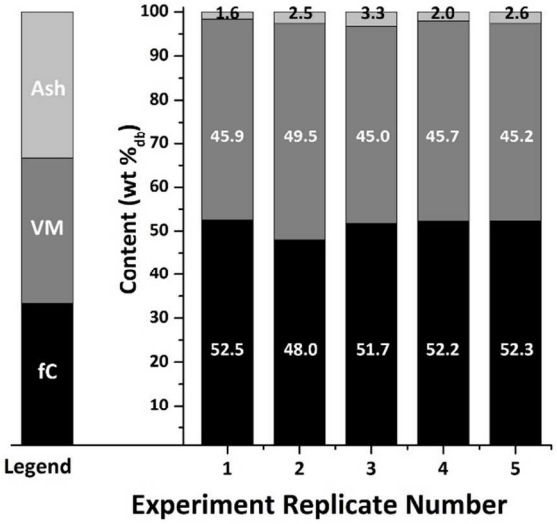

Figure 5. Reproducibility study on the proximate analysis of charcoals derived from spruce pyrolysis in the single WHTB at a heat treatment temperature of 300°C and an initial nitrogen pressure of 0.1 MPa.

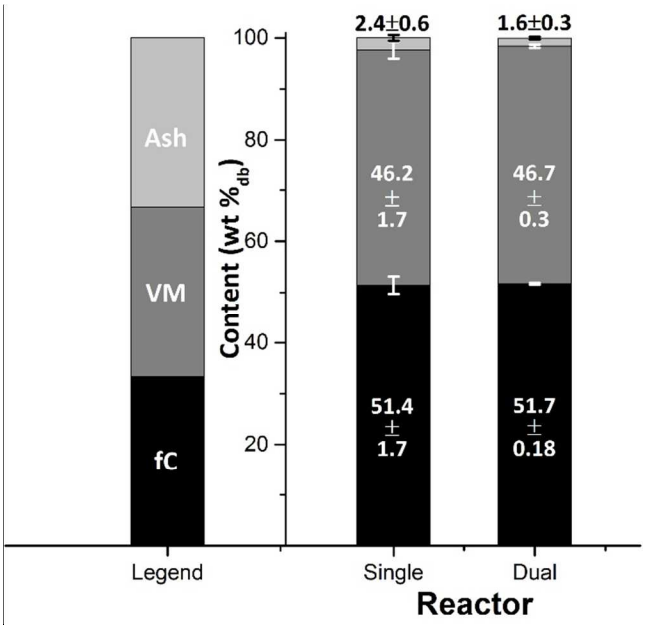

Figure 6. Comparison between proximate analyses of charcoals derived from spruce pyrolysis experiments in the single and dual WHTB at a heat treatment temperature of 300°C and an initial nitrogen pressure of 0.1 MPa.

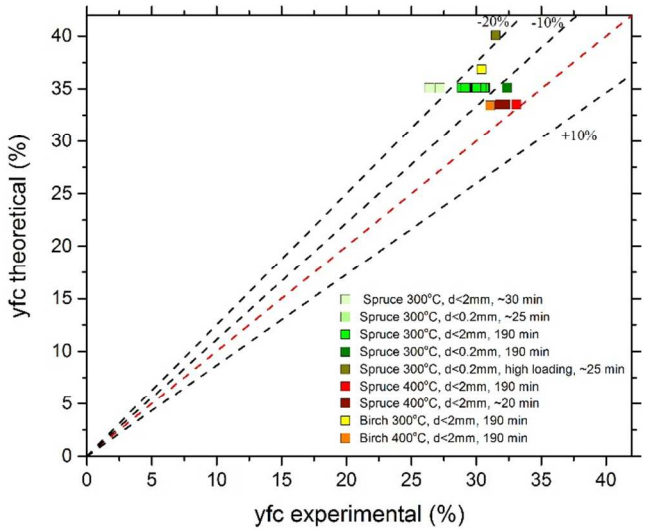

Figure 7. Parity plot showing experimental versus theoretical fixed carbon yields calculated with STANJAN.

This is the accepted manuscript of an article published in Energy & Fuels.
DOI: http://dx.doi.org/10.1021/acs.energyfuels.7b02982

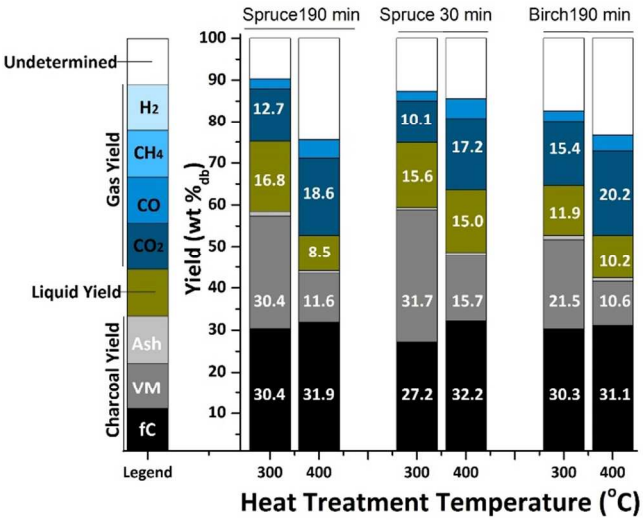

Figure 8. Effect of heat treatment temperature on the yields of char, condensate and gas from spruce and birch pyrolysis at an initial N_2 pressure of 0.1 MPa.

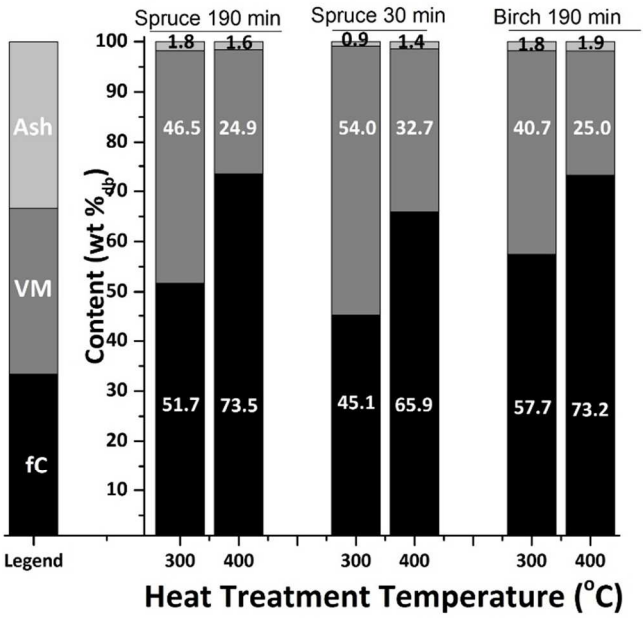

Figure 9. Effect of heat treatment temperature on the proximate analysis of charcoal from spruce and birch pyrolysis at an initial N_2 pressure of 0.1 MPa.

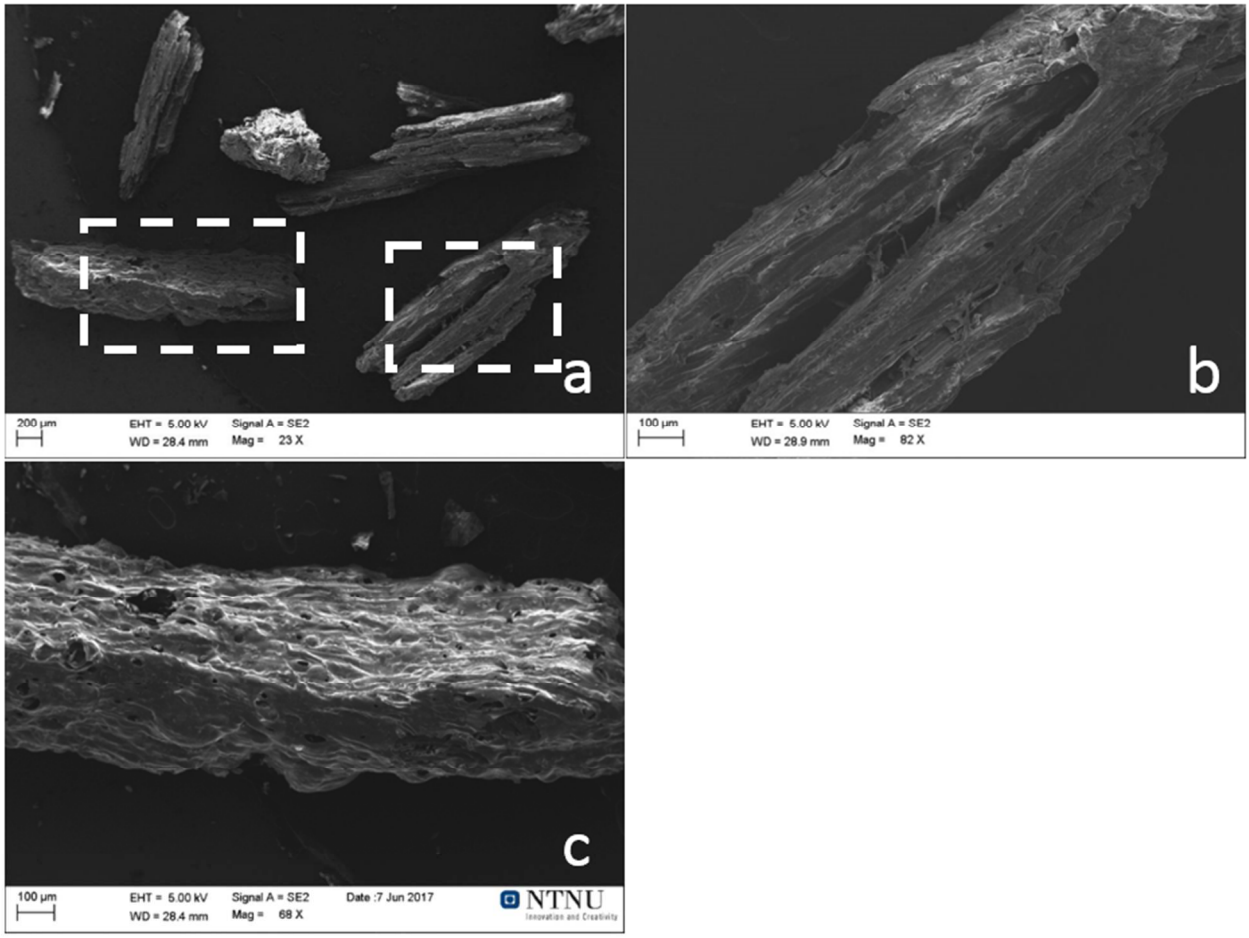

Figure 10. (a) SEM image of birch charcoal from experiment at a heat treatment temperature of 300°C and an initial nitrogen pressure of 0.1 MPa, (b) and (c) zoom-in views of selected areas in (a).

This is the accepted manuscript of an article published in Energy & Fuels.
DOI: http://dx.doi.org/10.1021/acs.energyfuels.7b02982

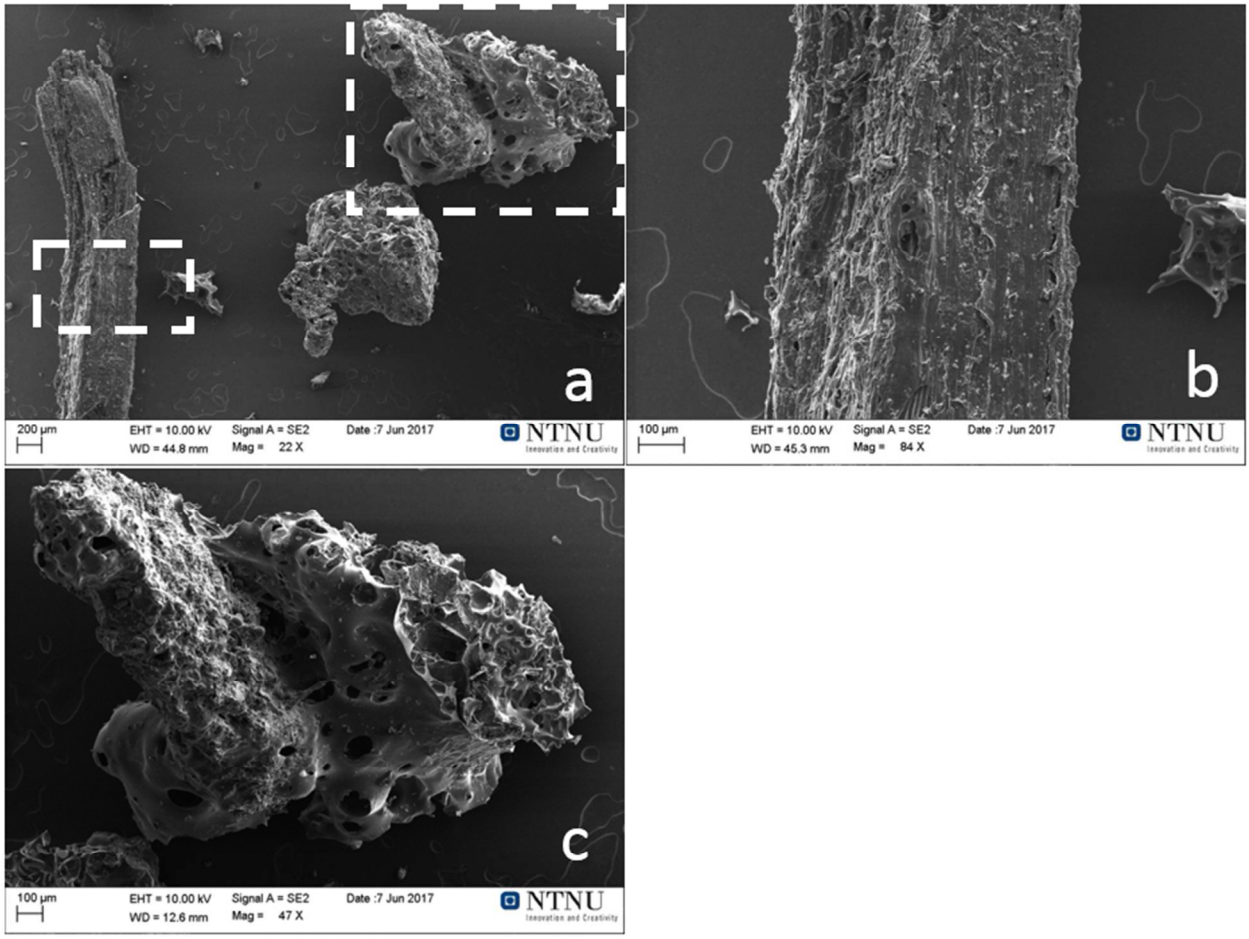

Figure 11. (a) SEM image of birch charcoal from experiment at a heat treatment temperature of 400°C and an initial nitrogen pressure of 0.1 MPa, (b) and (c) zoom-in view of selected areas in (a).

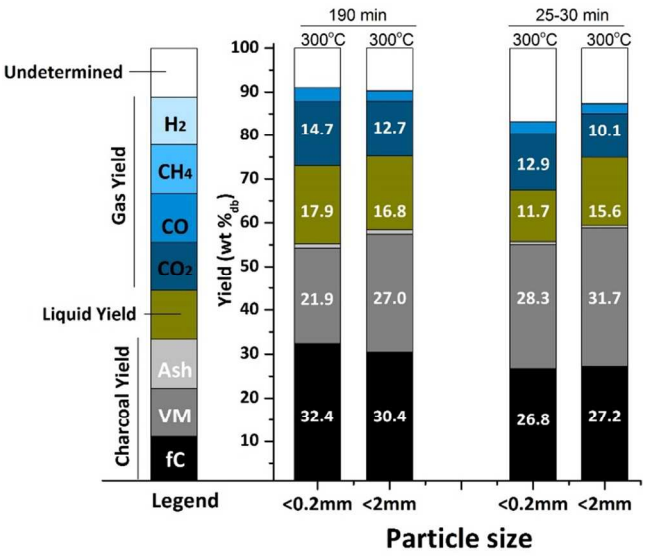

Figure 12. Effect of particle size on the yields of char, condensates and gas from spruce pyrolysis at a heat treatment temperature of 300°C and an initial nitrogen pressure of 0.1 MPa.

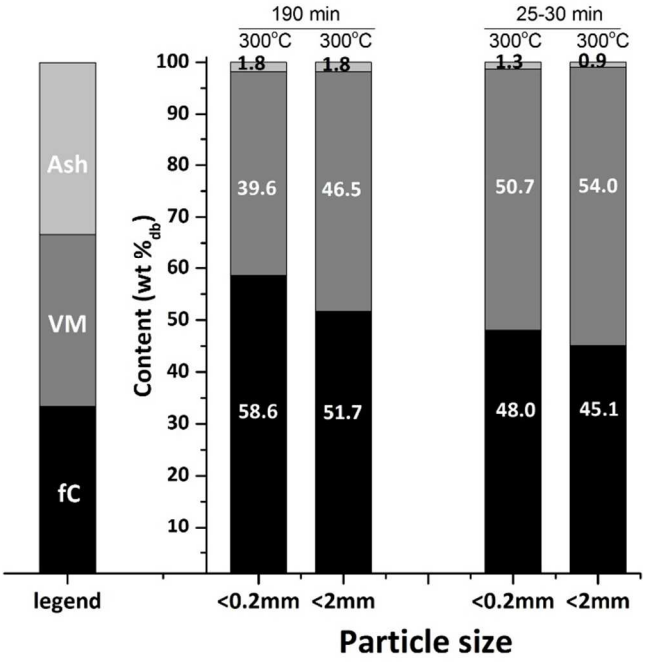

Figure 13. Effect of particle size on the proximate analysis of charcoal from spruce pyrolysis at a heat treatment temperature of 300°C and an initial nitrogen pressure of 0.1 MPa.

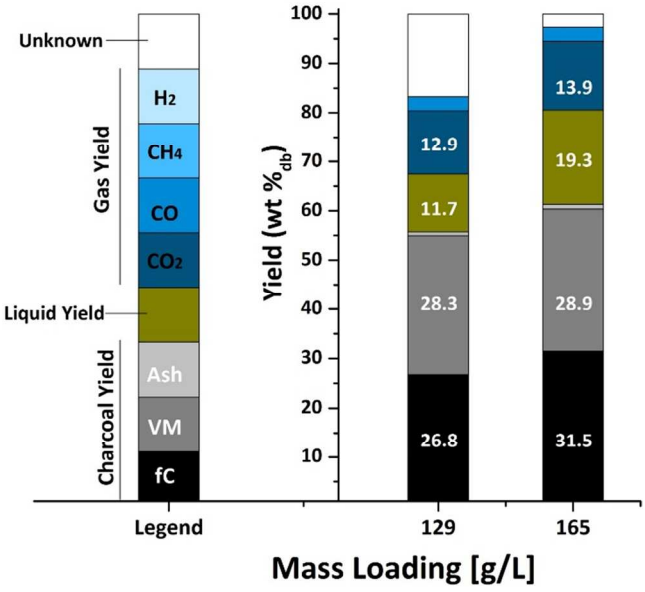

Figure 14. Effect of mass loading on the yields of char, condensates and gas from spruce pyrolysis at a heat treatment temperature of 300°C, an initial nitrogen pressure of 0.1 MPa, immersion time of around 25 minutes and sample size of <0.2 mm.

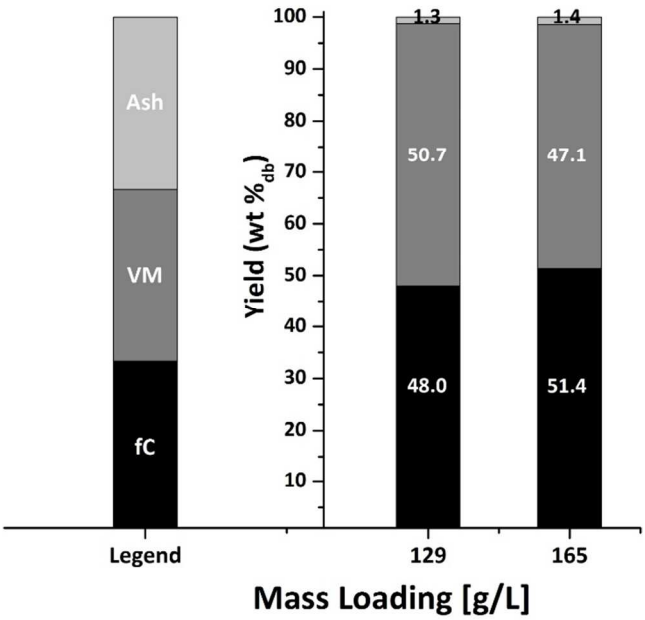

Figure 15. Effect of mass loading on the proximate analysis of charcoal from spruce pyrolysis at a heat treatment temperature of 300°C, an initial nitrogen pressure of 0.1 MPa, immersion time of around 25 minutes and sample size of <0.2 mm.

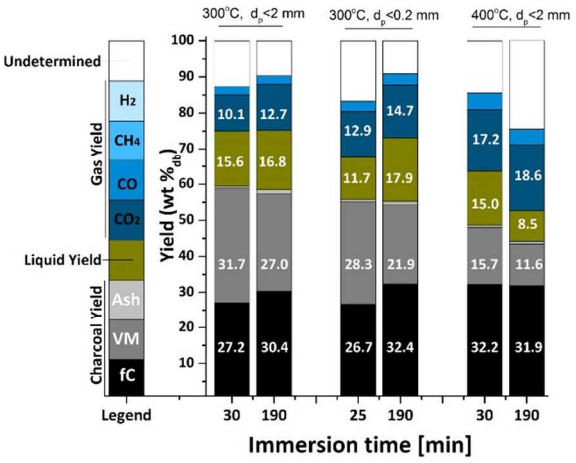

Figure 16. Effect of immersion time on the yields of char, condensates and gas from spruce pyrolysis at an initial nitrogen pressure of 0.1 MPa.

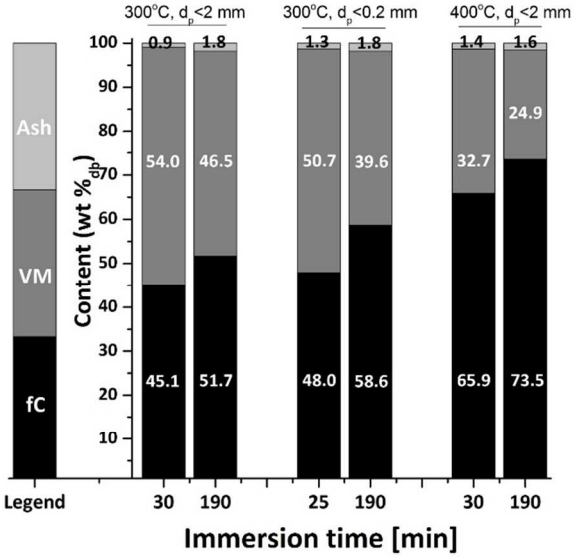

Figure 17. Effect of immersion time on the proximate analysis of charcoal from spruce pyrolysis at an initial nitrogen pressure of 0.1 MPa.

This is the accepted manuscript of an article published in Energy & Fuels.
DOI: http://dx.doi.org/10.1021/acs.energyfuels.7b02982

Table Captions

Table 1. Moisture content, elemental and proximate analysis of Norwegian spruce and birch feedstocks

Table 2a. Conditions and results for WHTB experiments at an initial pressure of 0.1 MPa of nitrogen.

Table 2b. Conditions and results for WHTB experiments at an initial pressure of 0.1 MPa of nitrogen.

This is the accepted manuscript of an article published in Energy & Fuels.
DOI: http://dx.doi.org/10.1021/acs.energyfuels.7b02982

Table 1. Moisture content, elemental and proximate analysis of Norwegian spruce and birch feedstocks

		Spruce	Birch
Moisture content [wt%, wet basis]		7.8	7.9
Ultimate Analysis[a] [wt%, dry basis]	C	46.93±0.05	47.4 ±0.3
	H	6.26±0.02	6.32±0.03
	O[c]	46.3	45.43
	N	0.20±0.02	0.20±0.02
	S	0.011±0.001	0.0158±0.001.
	Ash[d]	0.36±0.17	0.67±0.02
Proximate analysis[b] [wt%, dry basis]	fC[e]	14.8±0.1	13.1±0.2
	VM[f]	84.9±0.1	86.2±0.2
	Ash	0.36±0.17	0.67±0.02
Higher heating value [MJ/kg]		18.00	18.50

[a] Average of two samples, uncertainty indicates range of values
[b] Average of three analyses, uncertainty indicates standard deviation.
[c] Oxygen by difference.
[d] Determined by proximate analysis.
[e] Fixed-carbon content (fC).
[f] Volatile matter content (VM).

This is the accepted manuscript of an article published in Energy & Fuels.
DOI: http://dx.doi.org/10.1021/acs.energyfuels.7b02982

Table 2a. Conditions and results for WHTB experiments at an initial pressure of 0.1 MPa of nitrogen.

Experiment Number [#]	1-5[a,b,c]	6[a,b]	7[a,b]	8-9[a,c]		10		11		12	
Experimental Conditions											
Feedstock	Spruce	Oak	Cellulose	Spruce		Spruce		Spruce		Spruce	
Heat Treatment Temperature[°C]	300	300	300	300		300		400		300	
Immersion time [min][d]	190	190	190	190		190		190		28	
Mass Loading [$g_{biomass}/L_{reactor}$]	~100	~125	~205	~100		~130		~130		~130	
Particle size[mm]	<2	0.149-0.425	0.050-0.180	<2		<2		<2		<2	
Reactants				R1[e]	R2[f]	R1	R2	R1	R2	R1	R2
Moist Mass [g]	13.38	16.32	27.37	13.34	14.01	14.64	13.83	13.99	14.45	13.96	13.62
Moisture Content [%, wb[g]]	8.15	7.89	6.49	7.90		7.55		7.93		7.68	
Pyrolysis Reaction											
Axis Peak Temperature [°C]	317	380	552	310	317	317	336	427	499	318	325
Wall Peak Temperature [°C]	296	297	310	295	304	285	302	390	405	290	299
Peak Pressure [MPa]	2.63	3.54	7.09	2.72		4.65		7.74		3.95	
Solid Products											
Char Moist Mass [g]	10.84	12.95	13.58	8.87	11.91	10.44	11.21	8.30	7.46	9.37	11.38
Char Moisture Content [%, wb]	35.01	40.1	25.5	15.94	38.07	22.63	34.83	30.15	22.79	17.15	35.33
Volatile Matter Content [%, db[h]]	45.7	38.6	28.0	46.2	46.6	46.2	46.9	26.2	23.6	53.3	54.6
Ash Content [%, db]	2.0	3.6	0.2	2.1	1.4	1.8	1.7	1.7	1.5	0.9	1.0
Fixed Carbon Content [%, db]	52.2	57.4	71.8	51.7	52.0	52.0	51.4	72.1	75.0	45.8	44.4
Fixed Carbon Yield [%, db]	29.9	29.6	28.4	30.5	30.6	30.4	30.0	31.84	33.08	27.20	26.39
Higher Heating Value [MJ/kg]	28.92	28.23	31.13	28.52	28.77	28.79	30.83	31.92	35.03	31.06	27.81
Gas Products											
Final Gas in V_{Bomb} [mol][i]	0.054	0.073	0.143	0.117		0.119		0.195		0.099	
Nitrogen [mol %]	17.70	NA	NA	18.22		16.87		12.19		15.93	
Oxygen [mol %]	1.60	NA	NA	1.04		0.86		0.74		1.11	
Hydrogen [mg/g (Dry Feed)]	0.149	NA	NA	0.234		0.188		0.612		0.100	
Methane [mg/g (Dry Feed)]	0.00	NA	NA	0.01		0.00		0.00		0.00	
Carbon Monoxide [mg/g (Dry Feed)]	25.88	NA	NA	26.41		23.83		43.27		23.12	
Carbon Dioxide [mg/g (Dry Feed)]	114.11	NA	NA	118.21		127.23		185.68		100.81	
Mass Balance											
Gas Products [%, db]	14.01	NA	NA	14.49		15.13		22.96		12.40	
Char Yield [%, db]	57.32	51.59	39.53	58.88		58.44		44.14		59.39	
Liquid [%, db][j]	26.32	28.25	23.24	17.15		16.77		8.50		15.58	
Solid not recovered [%, db][k]								3.42		4.76	
Total [%, db]	**97.66**	**NA**	**NA**	**90.52**		**90.34**		**79.01**		**92.14**	
Carbon Balance Total [%, db]	**97.14**	**NA**	**NA**	**99.13**		**100.30**		**92.30**		**97.40**	

[a] Reactor with extended dead volume was employed.
[b] Single WHTB.
[c] Only the results of one of the replica experiments are displayed here.
[d] Long experiments are terminated 190 minutes after the WHTB is submersed into the hot sand bath. Short experiments finalize 10 minutes after the

This is the accepted manuscript of an article published in Energy & Fuels.
DOI: http://dx.doi.org/10.1021/acs.energyfuels.7b02982

end of the exotherm, i.e. the exotherm is considered to end once the pressure rise considerably slowed down.

[e] Data for reactor body 1 (R1) of the dual reactor.

[f] Data for reactor body 2 (R2) of the dual reactor.

[g] Reported on a wet basis(w.b.).

[h] Reported on a dry basis (d.b.).

[i] Final gas moles are calculated using the ideal gas law at conditions after cooldown. Final gas volume is measured with the WDV.

[j] Weight loss of char product from drying in a vacuum oven at 105°C.

[k] Amount of solid stuck on the walls is calculated as the initial and final masses of the empty reactors.

Table 2b. Conditions and results for WHTB experiments at an initial pressure of 0.1 MPa of nitrogen.

Experiment Number [#]	**13**		**14**		**15**		**16**		**17**		**18**	
Experimental Conditions												
Feedstock	Spruce		Spruce		Spruce		Spruce		Birch		Birch	
Heat Treatment Temperature[°C]	400		300		300		300		300		400	
Immersion time [min][d]	18		190		24		24		190		190	
Mass Loading [$g_{biomass}/L_{reactor}$]	~130		~130		~165		~130		~130		~130	
Particle size[mm]	<2		<0.2		<0.2		<0.2		<2		<2	
Reactants	R1	R2	R1	R2	R1	R2	R1	R2	R1	R2	R1	R2
Moist Mass [g]	14.60	14.27	13.87	14.48	19.48	17.84	14.22	14.01	14.34	14.01	14.62	14.22
Moisture Content [%, wb[g]]	7.77		7.52		7.11		7.02		7.88		7.98	
Pyrolysis Reaction												
Axis Peak Temperature [°C]	408	437	390	419	398	391	408	404	389	363	509	478
Wall Peak Temperature [°C]	394	395	302	301	294	299	301	299	296	298	392	393
Peak Pressure [MPa]	7.12		5.62		5.68		4.60		5.42		7.42	
Solid Products												
Char Moist Mass [g]	8.96	9.91	9.22	11.81	19.08	11.18	8.65	10.58	9.11	9.89	8.74	7.39
Char Moisture Content [%, wb]	27.30	35.11	22.38	38.03	45.19	3.65	19.07	27.88	25.23	29.57	35.02	24.40
Volatile Matter Content [%, db[h]]	32.3	33.1	39.6		47.1		50.7		40.7		25.0	
Ash Content [%, db]	1.5	1.3	1.8		1.4		1.3		1.8		1.9	
Fixed Carbon Content [%, db]	66.3	65.6	58.6		51.4		48.0		57.4		73.2	
Fixed Carbon Yield [%, db]	32.23	31.89	32.27		31.50		26.76		30.30		31.07	
Higher Heating Value [MJ/kg]	30.75	30.82	28.82		28.71		28.65		30.12		33.02	
Gas Products												
Final Gas in V_{Bomb} [mol][i]	0.173		0.132		0.152		0.116		0.129		0.196	
Nitrogen [mol %]	6.61		9.09		8.19		9.67		9.17		6.15	
Oxygen [mol %]	0.00		0.08		0.00		0.03		0.00		0.13	
Hydrogen [mg/g (Dry Feed)]	0.249		0.177		0.207		0.138		0.297		0.655	
Methane [mg/g (Dry Feed)]	0.00		0.00		0.00		0.068		0.00		0.00	
Carbon Monoxide [mg/g (Dry Feed)]	47.29		31.69		28.88		28.40		25.60		37.84	
Carbon Dioxide [mg/g (Dry Feed)]	171.93		147.03		138.64		129.42		154.33		202.20	
Mass Balance												
Gas Products [%, db]	21.95		17.89		16.77		15.80		18.02		24.07	
Char Yield [%, db]	48.62		55.21		61.24		55.74		52.75		42.45	
Liquid [%, db][j]	15.04		17.89		19.66		11.72		11.95		10.21	
Solid not recovered [%, db][k]	2.00		3.42		1.63		3.87		0.37		2.32	
Total [%, db]	**87.60**		**94.48**		**98.96**		**87.14**		**82.72**		**79.06**	
Carbon Balance Total [%, db]	**96.03**		**99.54**		**104.03**		**96.76**		**93.95**		**89.62**	

This is the accepted manuscript of an article published in Energy & Fuels.
DOI: http://dx.doi.org/10.1021/acs.energyfuels.7b02982

This is the accepted manuscript of an article published in Energy & Fuels.
DOI: http://dx.doi.org/10.1021/acs.energyfuels.7b02982